

Electronic Supplementary Information (ESI)

(C₃H₉NI)₄AgBiI₈: A Direct-bandgap Layered Double Perovskite Based on Short-chained Spacer Cation for light absorption

Yunpeng Yao,^{a,b,c} Bo Kou,^a Yu Peng,^{a,b,c} Zhenyue Wu,^a Lina Li,^a Sasa Wang,^{a,b}, Xinyuan Zhang,^{a,b} Xitao Liu,^{*a,d} and Junhua Luo^{*a}

^a State Key Laboratory of Structural Chemistry, Fujian Institute of Research on the Structure of Matter, Chinese Academy of Sciences, Fuzhou 350002, China, Email: Xitao Liu@fjirsm.ac.cn, jhluo@fjirsm.ac.cn.

^b University of Chinese Academy of Sciences, Beijing 100049, China.

^c School of Physical Science and Technology, Shanghai Tech University, Shanghai 201210, China

^d State Key Laboratory of Crystal Materials, Shandong University, Jinan, 250100, China

Experimental section

Materials and Synthesis

All chemicals were purchased by Aladdin except as otherwise noted. A reaction mixture, containing 3-Bromopropylamine hydrobromide (2.19 g, 10 mmol), Ag₂O (2.32, 10 mmol) and Bi₂O₃ (1.16 g, 2.5 mmol) in 50 mL of HI (47% in aqueous, including 0.5% H₃PO₂ is used to stabilize HI) solution at 373K at least 2 hours, after that the clarified liquid was slowly cooled to room temperature. Crimson crystals of **(C₃H₉NI)₄AgBiI₈ (IPAB)** was obtained.

Powder X-Ray Diffraction Analysis and Thermogravimetric Analysis

MiniFlex 600 Powder X-Ray Diffractometer (PXRD) was used to check the phase purity of desired compounds. The experimental PXRD patterns were recorded in the 2 theta (2θ) range of 5°-45° with a step size of 5°/min. The experimental PXRD patterns obtained at room temperature match well with the calculated data based on the single-crystal structure, which solidly confirm the purity of the as-grown crystals of **IPAB**. Thermogravimetric (TG) measurement was implemented on a *Netzsch STA 449C* thermal analyser with an N₂ flow rate of 30 mL min⁻¹ and a heating rate of 10 K min⁻¹ from 300 K to 1000 K.

Structure Determination

Single crystal X-ray diffraction (SCXRD) was performed on *Bruker D8* diffractometer by using Mo-Kα radiation (λ=0.71073 Å). Intensity data acquisition, data reduction and cell refinement were performed using the “multi-scan” program. The structures of all desired compounds were solved by direct methods and refinements were made by the least-squares program. Table S1 summarizes the detailed information of crystal parameters, structure refinement and data collection. The selected bond lengths and angles are shown in table S1-S2.

The refinement command “SIMU 0.005 0.01 2 C4 C5 C6 N2” and “SIMU 0.001 0.002 2 C1 C2 C3 N1” was used to limit the displacement of the C and N atoms.

Film fabrication

Dimethylformamide (DMF, Sigma-Aldrich, 99.8%, anhydrous), dimethylsulfoxide (DMSO, Sigma-Aldrich, 99.9%, anhydrous) were all used without further purification. Thin films were fabricated on fluorine doped tin oxide (FTO) coated glass substrates. The substrates were cleaned sequentially in hallmanex, acetone, isopropanol and O₂ plasma. The perovskite was deposited by spin-coating (speed = 4500 rpm, time = 25s) from a 60 wt% (DMF: DMSO = 3:1) solution of IPAB powders after heating to 100°C for 60 minutes. The resulting films were then annealed at 100 °C for 10 min. *Kw-4A* Spin Coater, *AS946C* specimen heating holder and *SC-UV-I* Ozone cleaner coming from *Beijing Coolcoater* was used in thin fabrications.

Elemental Analysis and Microstructure characterization

The mole ratio of C, H and N elements in **IPAB** was performed on *Vario EL-Cube* Elemental Analysis Instrument manufactured by Elementar. The Energy dispersive spectrometer (EDS) test were measured by Field Emission Scanning Electron Microscope *JSM6700-F* made by Japanese electronics and the result show the mole ratio of Ag, I and Bi are close to 1:12:1 which is on the match of the molecular formula of **IPAB**. *Ultima2* Inductively Coupled Plasma OES spectrometer (ICP) was used in measuring the ratio of Ag and Bi elements. The ICP result show the similar mole proportion of Ag and Bi (1:1) in **IPAB** compared with the EDS data. The Scanning Electron Microscope (SEM) images of thin films were measured by Field Emission Scanning Electron Microscope *SU-8010* made by Hitachi.

Ultraviolet-visible (UV-vis) Absorption Spectrum

UV-vis diffuse reflectance spectroscopy of desired materials was performed at room temperature on *Perkin-Elmer Lambda 900* UV-Vis spectrophotometer in a variable wavelength range between 200 to 1000nm. The BaSO₄ was used as the 100% reflectance reference, and the powdered crystals were used for the measurements.

Near the cut-off of the optical transmission, the band gap, the absorption and the wave frequency obey the equation: $\alpha h\nu = A (h\nu - E_g)^{n/2}$

where α , ν , A , and E_g are absorption coefficient, light frequency, proportionality constant, and band gap, respectively. In the equation, n decides the characteristics of the transition in a semiconductor ($n=1$, indirect absorption; $n=4$, indirect absorption). The values of n and E_g were determined by the following steps: first, plot $\ln(\alpha h\nu)$ vs $\ln (h\nu - E_g)$ using the approximate E_g value, and then determine the value of n with the slope of the straight line near the band edge; second, plot $(\alpha h\nu)^{1/n}$ vs $h\nu$ and then obtain the band gap E_g by extrapolating the straight line to the $h\nu$ axis intercept.

Computational Details

The structural and electronic properties of the layered double perovskite **IPAB** were calculated within the framework of density functional theory (DFT) by using the Vienna ab-initio simulation package (VASP) with the projector augmented wave (PAW) method. The generalized gradient approximation (GGA) within the Perdew-Burke-Ernzerhof (PBE) type exchange-correlation potentials, “intermediate” settings within FHI-aims and a (3 × 3 × 3) k-point grid was used throughout this work for **IPAB**. The following orbital electrons were explicitly treated as valence electrons: Ag, 4d¹⁰5s¹; Bi, 5d¹⁰6s²6p³; I, 5s²5p⁵; C, 2s²2p²; N, 2s²2p³ and H, 1s¹. Spin-orbit coupling (SOC) is included in a second-variational, non-self-consistent approach. The plane wave cutoff energy for the expansion of wave functions was set at 400 eV and the tetrahedron method with

Blöchl corrections was used for integrations. The numerical integrations in the Brillouin zones were performed on the Monkhorst-Pack k-meshes with the smallest spacing of 0.1 \AA^{-1} , which showed an excellent convergence of the energy differences (0.1 meV) and stress tensors (0.5 meV/\AA). The quasi-Newton algorithm as implemented in the VASP code was used in all structural relaxations.

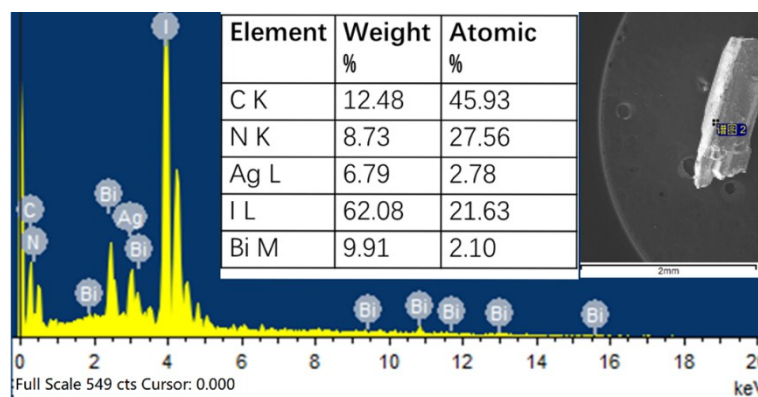


Figure S1. Energy dispersive spectrometer (EDS) spectrogram of compound **IPAB**.

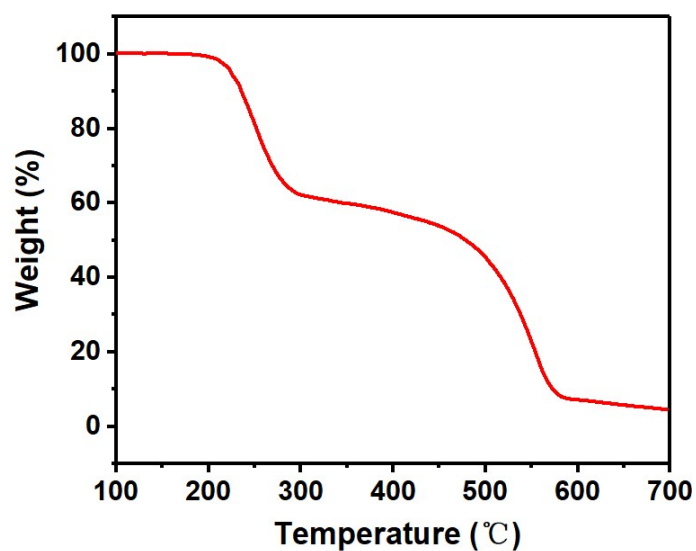


Figure S2. TGA patterns of **IPAB**.

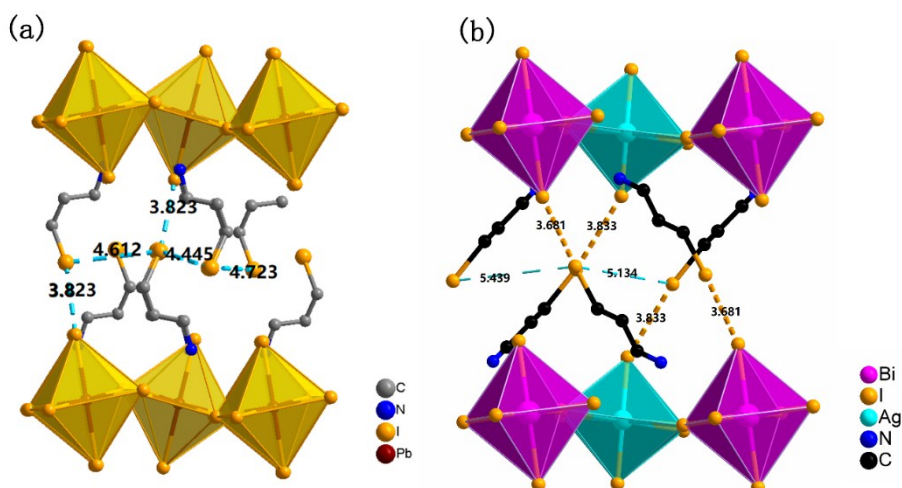


Figure S3. The distances between I atoms in $(\text{C}_3\text{H}_9\text{NI})_2\text{PbI}_4$ (a) and IPAB (b).

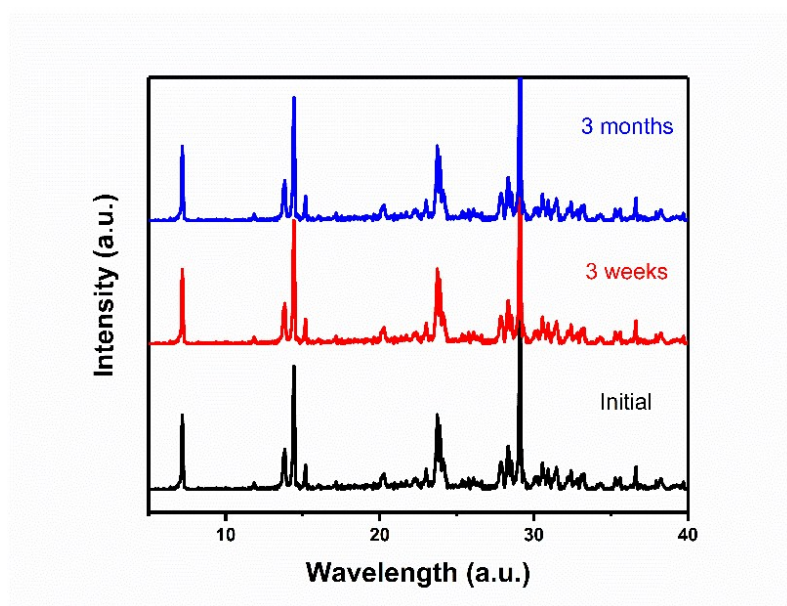


Figure S4. Air stability test of the IPAB.

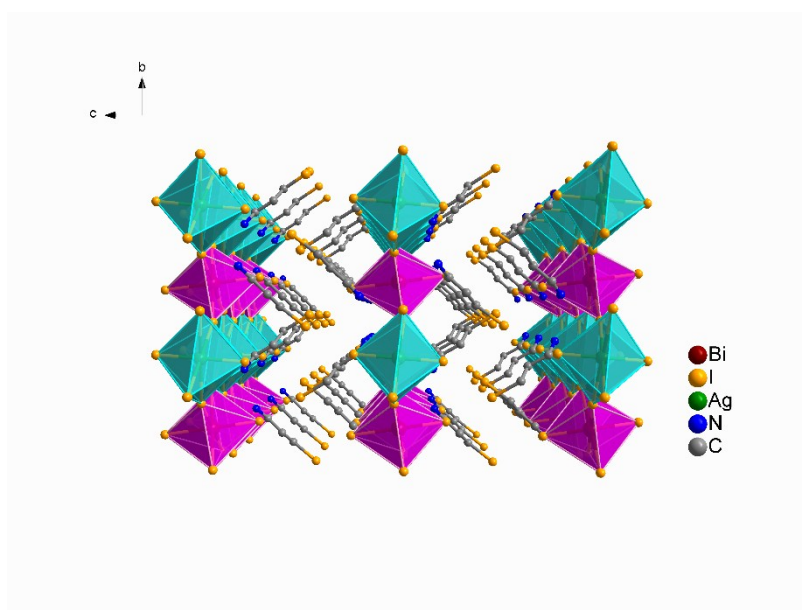


Figure S5. The packing diagram of IPAB. Hydrogen atoms were omitted for clarity.

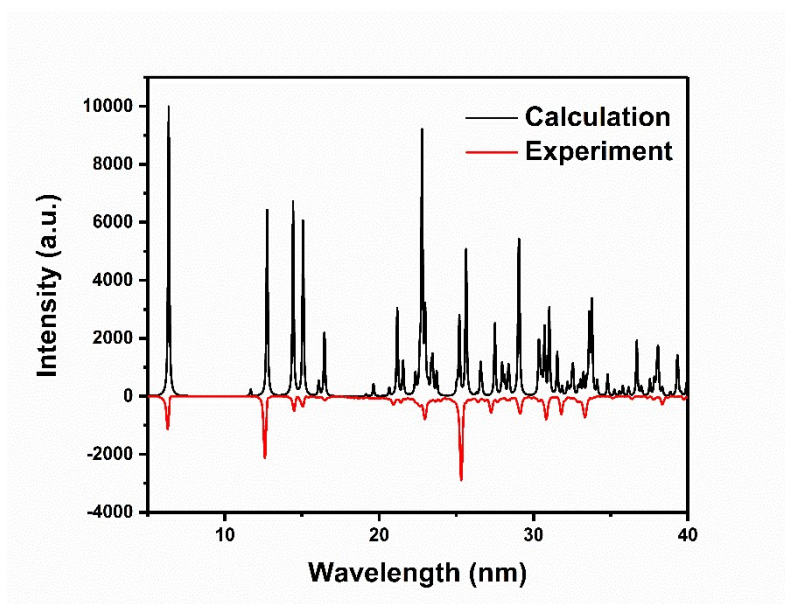


Figure S6. Powder X-ray diffractions patterns of $(\text{C}_3\text{H}_9\text{NI})_2\text{PbI}_4$.

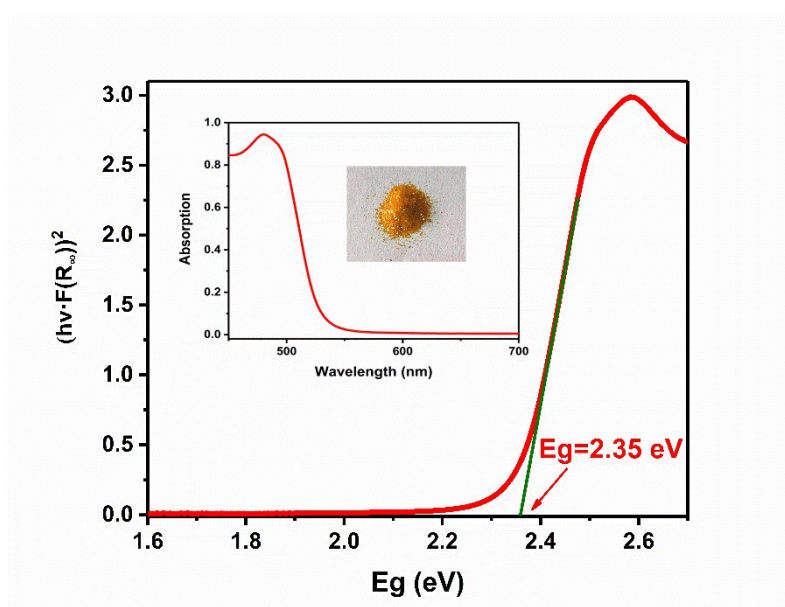


Figure S7. Corresponding Tauc plot of $(\text{C}_3\text{H}_9\text{NI})_2\text{PbI}_4$, insets show the absorbance spectrum of $(\text{C}_3\text{H}_9\text{NI})_2\text{PbI}_4$ and crystal colour.

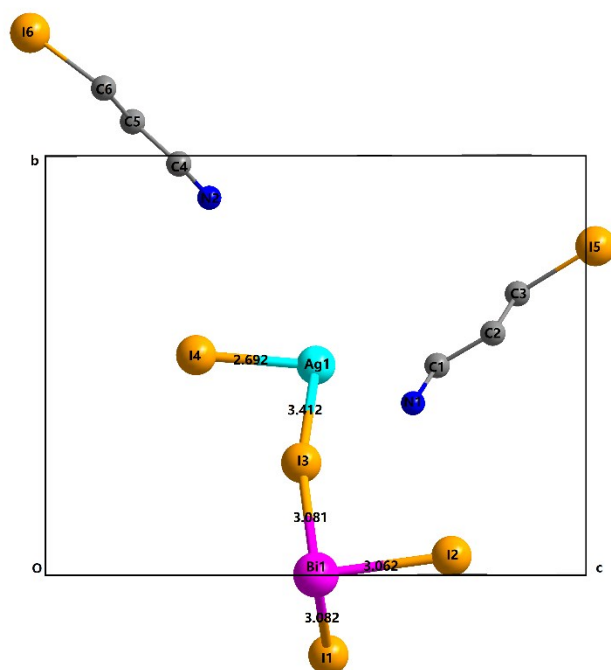


Figure S8. The asymmetric unit of IPAB. Hydrogen atoms were omitted for clarity.

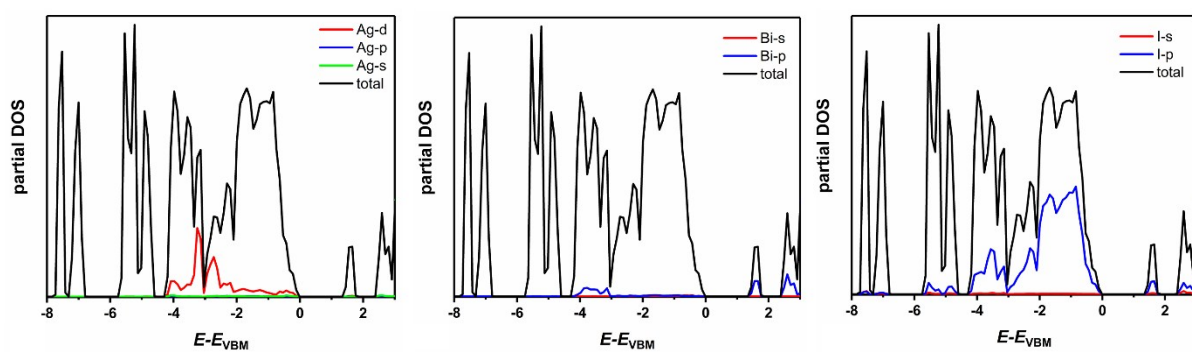


Figure S9. The partial DOS of IPAB for (d) Ag, (e) Bi and (f) I orbit.

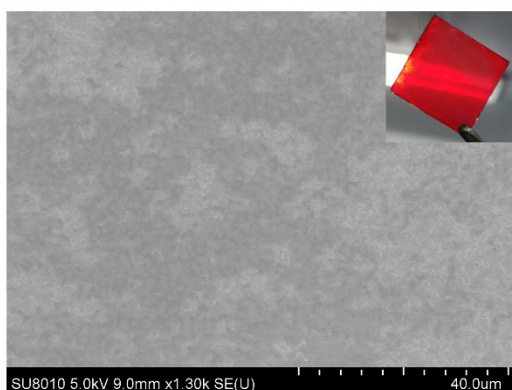


Figure S10. SEM images of the surface morphologies for thin films of IPAB and photograph of the thin film. Insert: color of IPAB thin film.

Table S1. Crystal data for **IPAB**.

Empirical formula	C ₁₂ H ₃₆ AgBiI ₁₂ N ₄
Formula weight	2076.10
Temperature/K	100.15 K
Crystal system	Triclinic
Space group	<i>P</i> $\bar{1}$
<i>a</i> /Å	8.6582 (5)
<i>b</i> /Å	9.3734 (6)
<i>c</i> /Å	12.1489 (8)
α /°	90.286 (3)
β /°	95.226 (2)
γ /°	90.478 (2)
Volume/Å ³	981.82(11)
Z	1
ρ_{calc} /cm ³	3.511
F (000)	902.0
limiting indices	-11 ≤ <i>h</i> ≤ 11, -12 ≤ <i>k</i> ≤ 12, -15 ≤ <i>l</i> ≤ 15
reflns collected	30969
completeness (%)	100
data / restraints / param	4318 / 36 / 141
final R indices [<i>I</i> > 2σ(<i>I</i>)]	R1 = 0.0576, wR2 = 0.1094
R indices (all data)	R1 = 0.0755, wR2 = 0.1175
^a R ₁ = Σ <i>F</i> _o - <i>F</i> _c / Σ <i>F</i> _o ; wR ₂ = {Σ [<i>w</i> (<i>F</i> _o ² - <i>F</i> _c ²) ²] / Σ <i>w</i> [(<i>F</i> _o) ²] ³ } ^{1/2}	

Table S2. Selected bond lengths (Å) and bond angles (°) for **IPAB**.

Bond	lengths (Å)	Bond	Angles (°)
Bi1-I1	3.0819(9)	I1-Bi1-I3	87.57 (2)
Bi1-I1 ¹	3.0819(9)	I2-Bi1-I3	87.57 (2)
Bi1-I2	3.0805(8)	I2-Bi1-I3	88.30 (2)
Bi1-I2 ¹	3.0805(8)	I2-Bi1-I1	91.09 (2)
Bi1-I3	3.0618(9)	I4-Ag1-I1	88.89 (2)
Bi1-I3 ¹	3.0618(9)	I1-Ag1-I1 ¹	180
Ag1-I1	2.6915(9)	I4 ³ -Ag1-I1	91.11 (2)
Ag1-I3	3.4175(9)	I4 ³ -Ag1-I2 ²	94.99 (2)
C3-I5	2.181(14)	I4-Ag1-I2 ²	85.01 (2)
C6-I6	2.150(14)	I2 ² -Ag1-I1	98.52
¹ 2-X,1-Y,2-Z		Ag1-I1-Bi3	155.64 (3)
		¹ 2-X,1-Y,2-Z; ² +X,-1+Y,+Z; ³ 1-X,-Y,2-Z	

Table S3. Several typical perovskites and their bandgap.

Perovskites	Bandgap (eV)	References
(BA) ₄ AgBiBr ₈	2.85	B. A. Connor, L. Leppert, M. D. Smith, J. B. Neaton and H. I. Karunadasa, J. Am. Chem. Soc., 2018, 140, 5235.
(C ₃ H ₉ Nl) ₂ PbI ₄	2.35	Lemmerer, Andreas, and David G. Billing. CrystEngComm 12.4 (2010): 1290-1301.
Cs ₂ AgBiBr ₆	2.1	E. T. McClure, M. R. Ball, W. Windl, P. M. Woodward, Chem. Mater. 2016, 28, 1348-1354.
[AE2T] ₂ AgBiI ₈	2	M. K. Jana, S. M. Janke, D. J. Dirkes, S. Dovletgeldi, C. Liu, X. Qin, K. Gundogdu, W. You, V. Blum and D. B. Mitzi, J Am Chem Soc, 2019, 141, 7955
(MA) ₂ AgBiBr ₆	1.95	Wei, F.; Deng, Z.; Sun, S.; Cheetham, A. K.; Zhang, F.; Evans, D. M.; Kieslich, G.; Tominaka, S.; Carpenter, M. A.; Zhang, J.; Bristowe, P. D. Chem. Mater. 2017, 29, 1089–1094.
(C ₆ H ₁₆ N ₂) ₂ AgBiI ₈ ·H ₂ O	1.93	L.-Y. Bi, Y.-Q. Hu, M.-Q. Li, T.-L. Hu, H.-L. Zhang, X.-T. Yin, W.-X. Que, M. S. Lassoued and Y.-Z.

		Zheng, Journal of Materials Chemistry A, 2019, 7, 19662.
--	--	---